Redesigning the coumarin scaffold into small bright fluorophores with far-red to NIR emission and large Stokes' shifts useful for cell imaging

Albert Gandioso,[†,‡] Roger Bresolí-Obach,[§] Alba Nin-Hill,[†,φ] Manel Bosch,[⊥] Marta Palau,[†] Alex Galindo,[†] Sara Contreras,[†] Anna Rovira,[†] Carme Rovira,[†,ξ,φ] Santi Nonell[§] and Vicente Marchán[†,‡,*]

[†]Secció de Química Orgànica, Departament de Química Inorgànica i Orgànica, Universitat de Barcelona, Martí i Franquès 1-11, E-08028 Barcelona (Spain)
E-mail: vmarchan@ub.edu

[‡]Institut de Biomedicina de la Universitat de Barcelona (IBUB), E-08028 Barcelona (Spain)

[§]Institut Químic de Sarrià, Universitat Ramon Llull, E-08017 Barcelona (Spain)

[φ]Institut de Química Teòrica i Computacional (IQTCUB), E-08028 Barcelona (Spain)

[⊥]Unitat de Microscòpia Òptica Avançada, Centres Científics i Tecnològics, Universitat de Barcelona, E-08028 Barcelona (Spain)

[ξ]Institució Catalana de Recerca i Estudis Avançats (ICREA), E-08010 Barcelona (Spain)

TOC ABSTRACT GRAPHIC

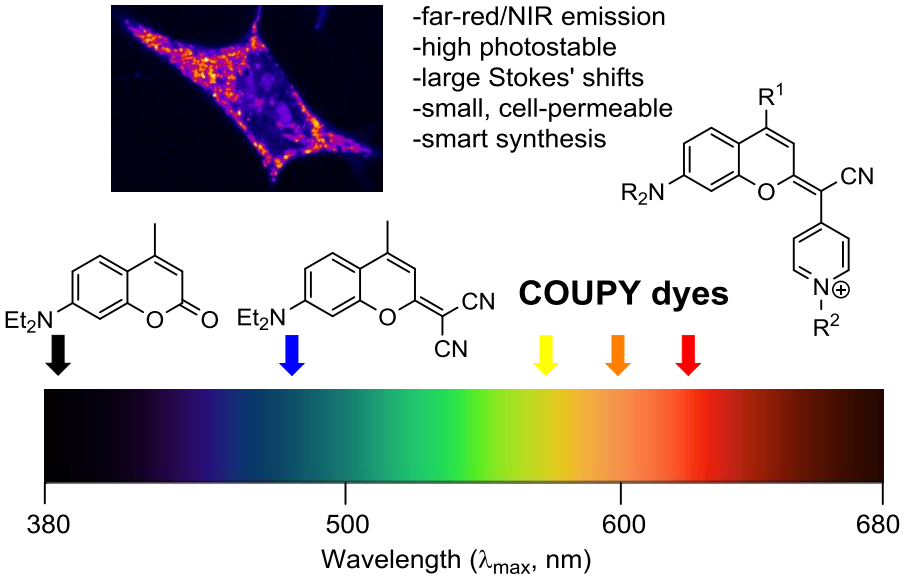

ABSTRACT

Among the palette of fluorescent organic molecules described up to now, coumarins are ideal candidates for developing cellular and molecular imaging tools due to their high cell permeability and minimal perturbation to the living system. However, blue to cyan fluorescence emission usually difficult *in vivo* applications due to the inherent toxicity and poor tissue penetration of short visible light wavelengths. Here we introduce a new family of coumarin-based fluorophores, nicknamed COUPY, with promising photophysical properties, including emission in the far-red/NIR region, large Stokes' shifts, high photostability, and excellent brightness. COUPY fluorophores were efficiently synthesized in only three linear synthetic steps from commercially available precursors, the *N*-alkylation of a pyridine moiety being the key step at the end of the synthetic route since it allows to tune the photophysical properties of the resulting dye. Owing to their low molecular weight, COUPY dyes show excellent cell permeability and accumulate selectively in nucleoli and/or mitochondria of HeLa cells, being their far-red/NIR fluorescence emission easily detected at a concentration as low as 0.5 μM after incubation for only 20 min. We anticipate that these coumarin scaffolds will open the way to the development of novel coumarin-based far-red to NIR-emitting fluorophores with potential applications for organelle imaging and biomolecule labelling.

INTRODUCTION

Fluorophores based on organic molecules are powerful tools in modern cellular and molecular imaging techniques as well as for the *in vivo* detection and/or quantification of biologically relevant species.[1] Among them, far-red and near-infrared (NIR) fluorophores are particularly interesting since emission at longer wavelengths exhibits several appealing features such as deep tissue penetration, minimal autofluorescence interference and low light scattering, while minimizes photodamage to living cells compared with UV and blue light.[2] Despite the large number of far-red/NIR fluorescent dyes described up to now, most of them are far from being ideal due to sub-optimal photophysical parameters (e.g. small Stokes shifts and poor photostability) and physico-chemical properties (low aqueous solubility, undesirable aggregation)[3] due to their large size and structural complexity, the latter being a consequence of the necessity of extending π-conjugation to red-shift absorption and emission. Most commercially available far-red or NIR fluorophores are derived from cyanines,[4] which are also highly polar, making them cell impermeable and not completely suitable for use in live cells. Consequently, it is urgent to develop new fluorophores based on low molecular-weight scaffolds operating in the optical window of the tissues with high cell permeability and minimal perturbation to the living system.[5] Ideally, such small scaffolds should be amenable to smart structural modifications to easily tune their absorption/emission properties on demand, preferably at the late synthetic stages,[6] as well as for facilitating conjugation to biomolecules such as lipids, peptides, proteins, oligonucleotides or antibodies.

Among the palette of fluorescent organic molecules,[1,3a] coumarin scaffolds are ideal candidates for this purpose owing to their good cell membrane permeability and well-stablished photophysical properties. The fluorescence emission of the basic coumarin scaffolds (e.g. compound **1** in Scheme 1, usually referred to as Coumarin 1) can be shifted from blue to cyan by incorporating electron-donating groups at position 7 of the coumarin skeleton (e.g. *N*,*N*-dialkylamino or hydroxy/alkoxy) that partner with the electron-withdrawing lactone moiety to create a push-pull effect. Based on this premise, great efforts have been devoted to red-shift the emission of coumarins by introducing additional electron-withdrawing groups

(EWG) at positions 3 and/or 4 (CN, CF_3, carboxyl), by extending the π–conjugation system through position 3 with methine, carbonyl o heteroaryl linkages,[7] or by fusion of aromatic cycles,[8] including other fluorescent scaffolds such as rhodamine[9] or BODIPY.[7b,10]

Despite huge synthetic efforts dedicated to the coumarin scaffold, little work has been devoted to modifying the lactone function. Thionation of the carbonyl group (e.g. compound **2** in Scheme 1) is known to cause significant red-shift, leading to blue absorption (λ_{max} ~470 nm) and green light emission (λ_{em} ~550 nm) in the 7-*N*,*N*-diethylamino series.[11] Similarly, extending the conjugation of the system at position 2 via the incorporation of a dicyanomethylene group (e.g. compound **3** in Scheme 1) has been reported to induce similar bathochromic effects both in absorption and in emission in several systems,[12] including dicyanocoumarin-caged morpholino oligonucleotides[12c] and RGD-containing peptides.[12d] Very recently, we have reported for the first time the synthesis of coumarin derivatives in which one cyano group in coumarin **3** was replaced by a phenyl ring containing EWGs at *ortho* and *para* positions to increase the push-pull character of the chromophore (e.g. compound **4** in Scheme 1).[13] Although such modifications red-shifted absorption into the green to red region and allowed to obtain new caging groups photoremovable with visible light, the incorporation of several strong EWGs such as nitro was found to have a negative effect on the fluorescence emission of the compounds.[13]

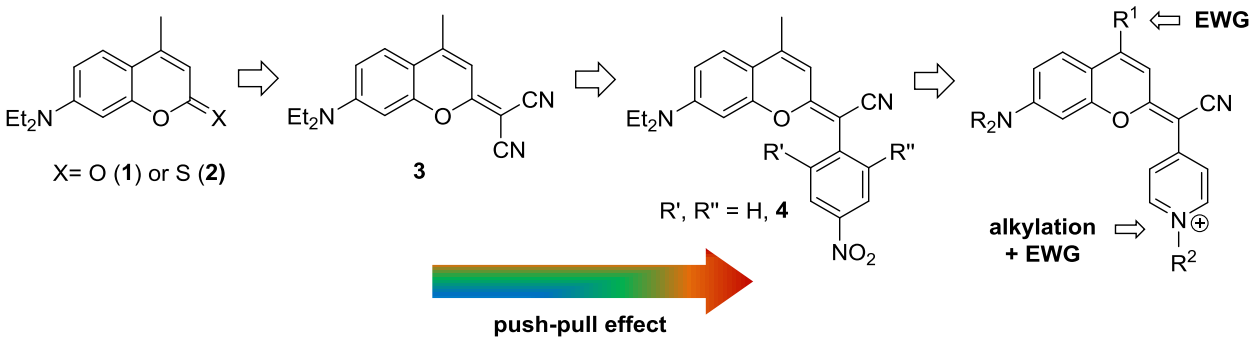

Scheme 1. Rational design of the new coumarin-based fluorophores synthesized in this work.

With the aim of further red-shift absorption and emission of the coumarin scaffold while keeping a low-molecular weight, we focused on replacing one cyano group in the dicyanomethylenecoumarin **3** by pyridine (Scheme 1). We reasoned that this modification could increase the π-conjugation and the push-pull character of the chromophore, which would result in a large bathochromic shift in absorption and emission bands. The electron-deficient pyridine heterocycle offers many other attractive features, such as the possibility of tuning its electronic properties through the incorporation of EWG substituents as well as *N*-alkylation. The latter is an important advantage since the resulting positive charge on the nitrogen atom would lead to an increased electron-withdrawing effect and, consequently, to a large intramolecular charge-transfer effect along the coumarin skeleton. Based on this rational design, here we introduce a new family of coumarin-based fluorophores, nicknamed COUPY, which shows promising photophysical properties, including large Stokes' shifts, large photostability, brightness and emission in the far-red/NIR region. Importantly, their photophysical properties were easily tuned by selecting the appropriate combination of the *N*-alkylating group at the pyridine moiety (CH_3 or CH_2CF_3) and the substituent at position 4 (CH_3 or CF_3), while keeping a low molecular weight (M.W. 340-440) and rapid access in only three linear synthetic steps from cheap commercially available precursors. Moreover, excellent cell permeability was found in HeLa cells, where the compounds accumulated selectively in nucleoli and/or mitochondria.

RESULTS AND DISCUSSION

Design, synthesis and characterization of COUPY scaffolds

The synthesis of the new fluorophores was designed from commercially available Coumarin 1 (**1**) (Scheme 2). We also selected Coumarin 152 (**5**) because the incorporation of strong EWGs such as CF_3 at the position 4 of the coumarin skeleton is known to increase the photostability of the dye when compared with the unsubstituted derivative,[14] and to induce a pronounced red-shift of the absorption and emission bands by enhancing its "push-pull" character.[7bc,15] This modification has been applied in a coumarin-based commercially available dye (AlexaFluor 430) and in the xanthene skeleton for developing deep-red and NIR dyes.[9b,16] Since we and others have demonstrated the utility of thiocoumarin derivatives to introduce the dicyanomethylene functionality within the coumarin skeleton,[12bcde] we first synthesized thiocoumarins **2**[13] and **6** by reaction with Lawesson's reagent (LW, Scheme 2). To our delight, condensation with 4-pyridylacetonitrile in the presence of a strong base followed by treatment with silver nitrate afforded coumarins **7** and **8** in excellent yields after silica column chromatography (89 % and 84 %, respectively). Full characterization was carried out by high resolution ESI mass spectrometry and NMR (^1H, ^{13}C and ^{19}F) and the purity was assessed by reversed-phase HPLC-MS (Figure S1), revealing a single peak in both cases.

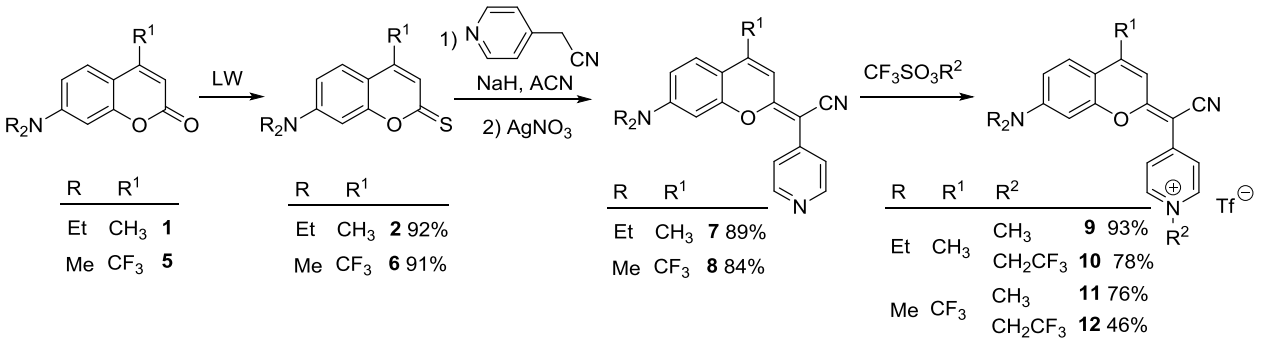

Scheme 2. Synthesis of coumarin fluorophores **9-12**.

Interestingly, the ^{1}H NMR spectrum of coumarin **7** showed the presence of two sets of proton signals in $CDCl_3$ and in DMSO-d_6 in an ~ 90:10 ratio (see Figure 1), and the same duplicity was found in the ^{13}C NMR spectra. Full assignment of the ^{1}H NMR spectrum by using 2D COSY and NOESY experiments (Figures 1 and S3-S4) confirmed the presence of two species in slow equilibrium in solution on the chemical shift time scale. As shown in Figure 1B, the presence of chemical exchange cross-peaks between the resonances of the two species in the 2D NOESY spectrum accounts for the existence of *E* and *Z* interconverting rotamers around the exocyclic C=C bond with an exchange rate (k_{ex}) of approximately <10 s^{-1}. It should be mentioned that noticeable exchange cross-peaks were only observed in DMSO-d_6 and not in $CDCl_3$. Further evidence of the dynamic interconversion of the two species was provided by 1D-selective chemical exchange experiments (Figure 1C).[17] The existence of rotamers instead of diastereomers can be attributed to the strong push-pull character of the compounds: the exocyclic C=C bond connecting the C-2 of the coumarin moiety and the C-4 of the pyridine cannot be considered a pure double bond but a double bond with partial single bond character due to π-delocalization. The presence of diagnostic NOE cross-peaks such as the one between H3 proton of the coumarin in the minor rotamer and the meta protons of the pyridine (Figure 1) allowed to conclude that the *E* rotamer was the one preferred (as usually drawn in the manuscript). A similar behavior was found for the 4-trifluoromethylcoumarin analogue (**8**), in which an ~ 93:7 mixture of the two rotamers was identified in solution by NMR (Figures S5-S6). Again, ^{1}H-^{1}H NOESY experiments allowed to conclude that the *E* rotamer was the major species in solution.

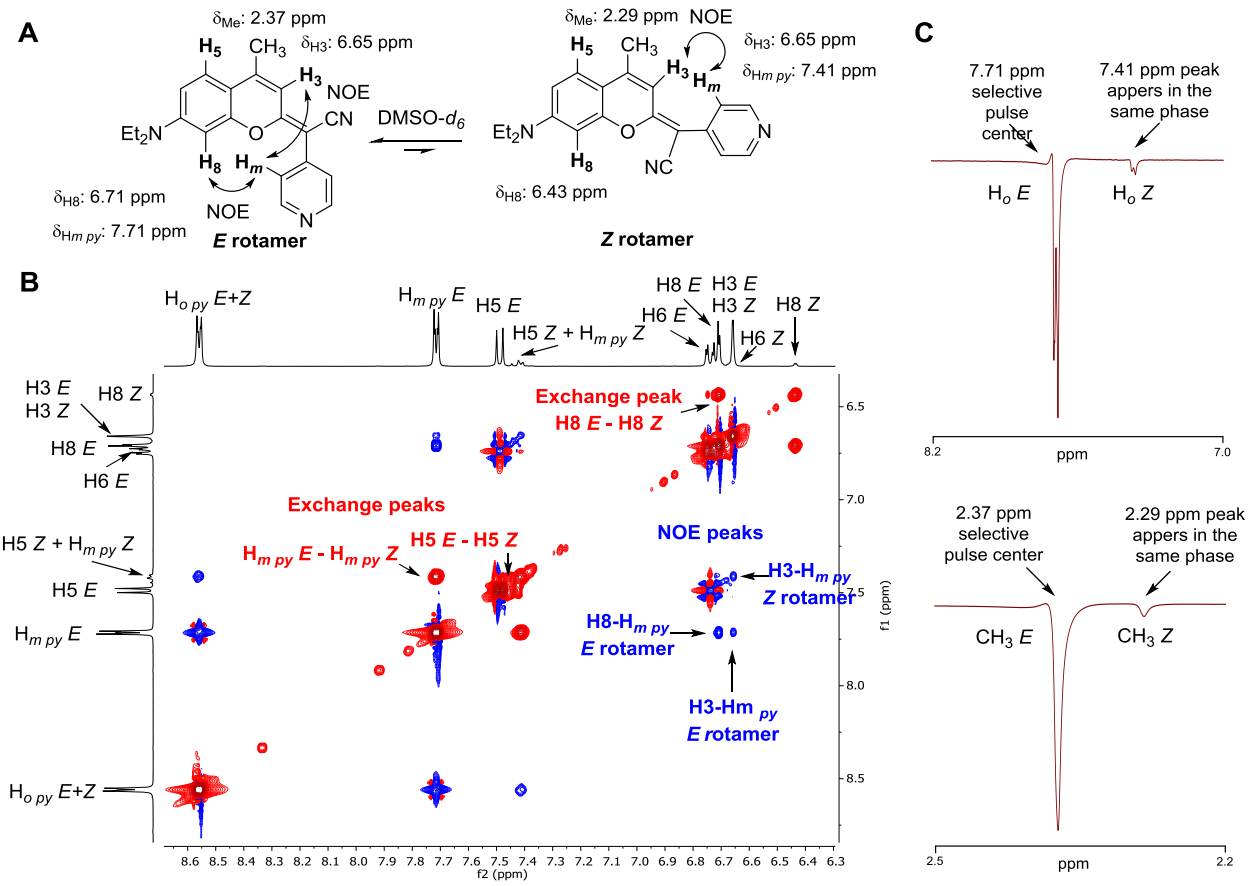

Figure 1. A) Structure of *E* and *Z* rotamers of coumarin **7** with some diagnostic NOE cross-peaks indicated. B) Expansion of the 2D NOESY spectrum (t_m = 500 ms, 25ºC) of **7** in DMSO-d_6 showing exchange cross-peaks between rotamer resonances of the same sign as the diagonal. C) 1D gradient NOE spectrum of coumarin **7** with an initial selective pulse at 7.71 ppm (top) or at 2.37 ppm (bottom) conduces to new peaks of the same phase at 7.41 ppm or at 2.39 ppm, respectively, implying chemical exchange and, for instance, the existence of rotamers.

Having stablished by NMR the existence of rotamers in solution for the two coumarin scaffolds, we decided to get some more insights on these experimental observations from a theoretical point of view. DFT calculations were carried out with the Gaussian09 (G09) software package (see Figures S11-S16 and Tables S1-S5 in the Supporting Information). As shown in Figure 2, the core of the coumarin scaffold **7** is essentially planar in the optimized structures of the two rotamers, being the pyridine moiety slightly twisted. The C-C and C-N bond lengths determined by DFT calculations confirmed the strong electronic

delocalization along the π-conjugated system, from the electron-donating NEt_2 group to the pyridine and nitrile. Notably, the value of the exocyclic C=C bond length (1.40 Å) is the intermediate between a single (1.45 Å) and double (1.33 Å) Csp^2-Csp^2 bond (Table S3). The calculated rotational energy barrier (19.6 kcal/mol, Figure 2C) enables interconversion under normal conditions, and the calculated probability of obtaining *E* and *Z* rotamers was approximately 84% and 16%, respectively, which is in good agreement with the experimental ratio determined by NMR. Moreover, a good correlation between the charges of the atoms calculated using the electrostatic potential (ESP) fitting method (Table S4 and Figure S13) and the expected electronic delocalization of the system was found.

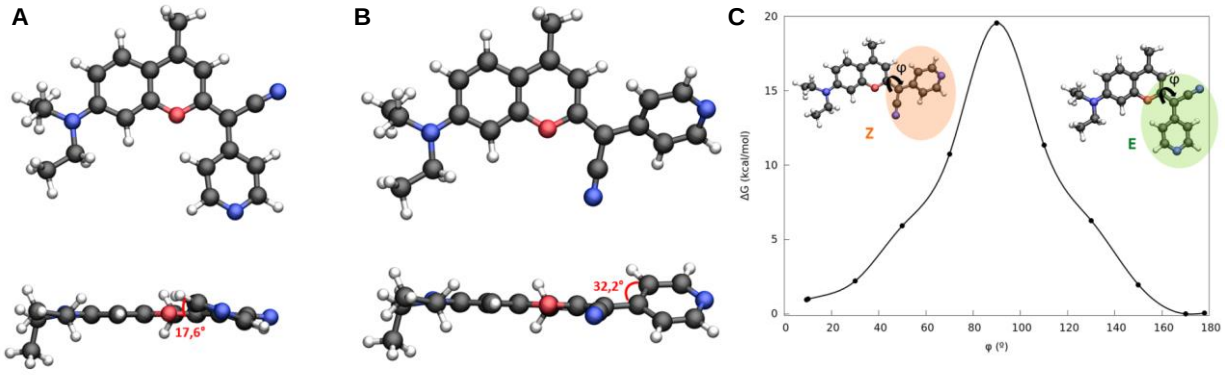

Figure 2. DFT optimized structures of rotamers *E* (A) and *Z* (B) of coumarin **7**, and energy profile resulting from rotating the φ dihedral angle, from the *Z* rotamer to the *E* rotamer (C).

Synthesis and photophysical characterization of COUPY fluorophores

To our delight, analysis by UV-HPLC-MS of coumarin derivatives **7** and **8** (Figure S1) revealed a strong bathochromic shift (63 and 85 nm, respectively) of their absorption maximum compared with that of the parent dicyanocoumarin **3** (λ_{max} = 478 nm in **3** *vs* λ_{max} = 541 nm in **7** and λ_{max} = 563 nm in **8**) and even with respect coumarin **4** (λ_{max} = 499 nm).[13] This red-shift can be attributed to the increased push-pull character of the conjugated π-electron system of the chromophore due to the replacement of the nitrile group in **3** or the *p*-nitrophenyl in **4** by pyridine, which was assumed to be protonated during HPLC analysis under acidic conditions (0.1% trifluoroacetic acid). Such encouraging results led us to synthesize *N*-alkylated pyridinium analogues to obtain pH-independent fluorophores based on the two COUPY

scaffolds. As shown in Scheme 2, reaction of **7** with methyl trifluoromethanesulfonate afforded *N*-methylpyridinium-coumarin derivative **9** as a purple solid with excellent yield and purity after a simple precipitation without the need of further purification. Using this simple method, we readily prepared coumarin **10** by using the commercially available 2,2,2-trifluoroethyl trifluoromethanesulfonate as alkylating reagent with the aim of causing an additional red-shift of the maximum absorption because of the strong electron-withdrawing character of the CF_3 group. Following the optimized procedures, we synthesized the 4-trifluoromethyl analogues **11** and **12** from coumarin scaffold **8** (Scheme 2). The four new coumarin derivatives were isolated as purple (**9-11**) and dark blue solids (**12**) and fully characterized by HR ESI-MS and 1D (^{1}H, ^{13}C and ^{19}F) and 2D NMR, and their purity was assessed by HPLC analysis (Figure S2). It is worth noting that the *E* rotamer was the major species in solution for coumarin derivatives **9**, **10** and **12** as inferred by 2D NOESY experiments (Figures S7-S10), while 8% of rotamer Z was identified in solution for coumarin **11**.

Having at hand four new coumarin derivatives, we investigated their photophysical properties (absorption and emission spectra, molar absorption coefficients (ε), fluorescence quantum yields (Φ_F) and fluorescence life-time (τ_F)) in several solvents of different polarity and viscosity (H_2O, phosphate buffer saline (PBS), methanol (MeOH), glycerol, acetonitrile (ACN), dichloromethane (DCM) and toluene). The UV-Vis absorption and emission spectra are shown in Figure 3 and Figures S17-S18 and their photophysical properties are summarized in Tables 1 and S6. All the compounds showed an intense absorption band in the yellow-red part of the visible spectrum, with absorption maxima ranging from 569 nm (**9**, DCM) to 621 nm (**12**, DCM), which provided intense coloured solutions (Figure 3). As expected, from **7-8** coumarin derivatives, replacement of the CH_3 group at position 4 of the coumarin skeleton by the strong electron-withdrawing CF_3 caused a significant red-shift (from 21 to 33 nm, depending on the solvent) in the absorption maximum wavelength. A similar effect was observed when comparing *N*-methylated compounds with the corresponding *N*-trifluoroethylated analogues, as exemplified by the far-red absorption of the compound containing two CF_3 groups (**12**). The position of the maxima for the *N*-methylated compounds were not modified by changing the pH beyond a small shift (Figure S19). By

contrast, the spectroscopic properties of the non-methylated compounds, e.g. **7**, were strongly influenced by the pH of the media, which correlates well with the protonation state of the pyridine moiety. However, the striking observation was made that all the compounds showed negative solvatochromism, i.e., the absorption maxima shifted to the blue when increasing solvent polarity (e.g. for **9**: λ_{abs} = 543 nm in H_2O and 569 nm in DCM) which sets them apart from conventional coumarin derivatives.[18] This suggests that COUPY dyes have a smaller dipole moment in the excited state than in the ground state, in agreement with the computational results (Figure S13). For **9**-**12**, the difference between the ground and excited state dipole moments is in the range -4.8 to -6.1 D (Table S6 and Figure S21).[19] The molar absorption coefficients (ε) were also influenced by the polarity of the solvent, showing hyperchromism in less polar solvents, and by the nature of the R^1 substituent: 4-CF_3 coumarins exhibited smaller ε values than the 4-CH_3 analogues.

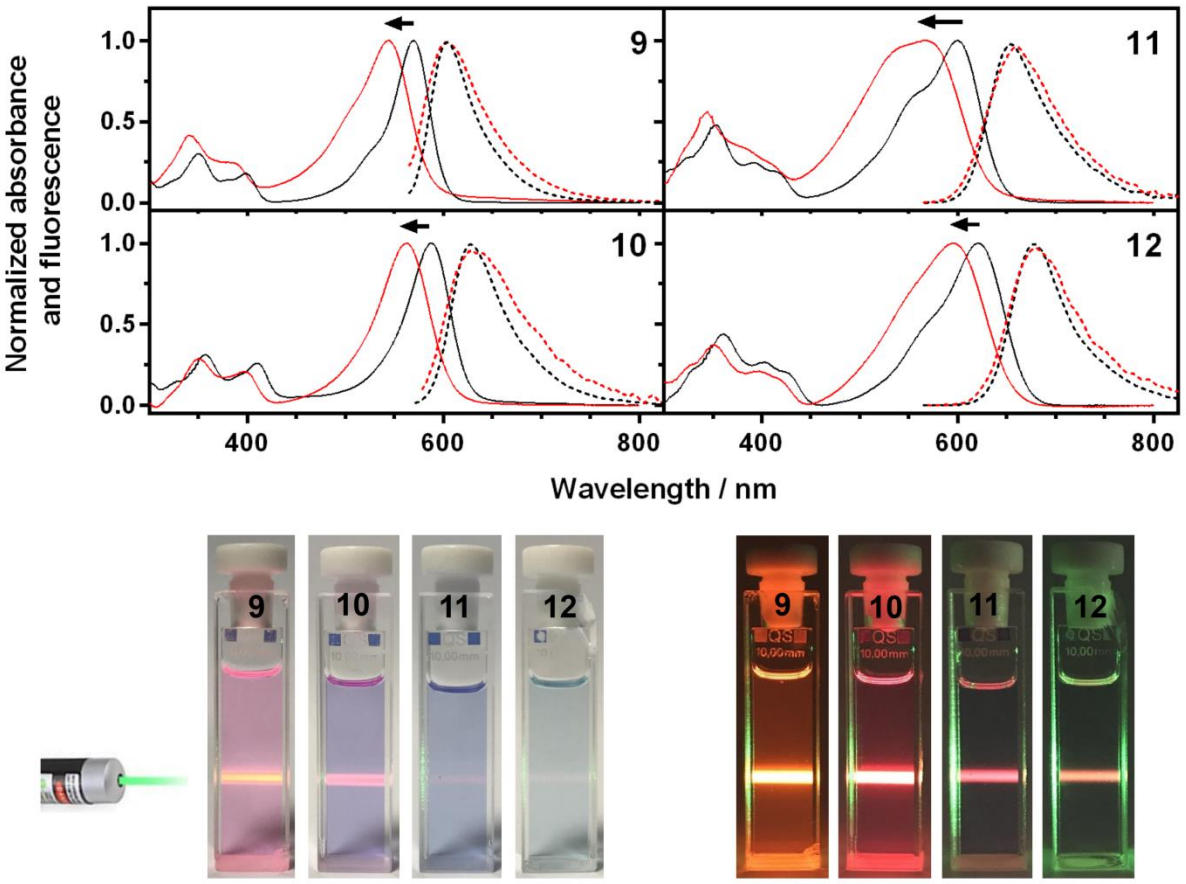

Figure 3. Top: Comparison of the normalized absorption (solid lines) and fluorescence (dotted lines) spectra of COUPY dyes (compounds **9-12**) in DCM (black lines) and in H_2O (red lines). Bottom: Photographic images of coumarin derivatives **9-12** (5 μM) in DCM under day light (left) and in the dark (right) upon irradiation with green light laser (532 nm).

Very interestingly, coumarin derivatives **9-12** showed emission in the far red to NIR region (Figures 3 and S18), with emission maximum ranging from 609 nm (**9**, ACN) to 689 nm (**12**, ACN), which again demonstrated that the incorporation of CF_3 groups into the coumarin skeleton was highly positive for red-shifting the emission. In contrast with absorption maxima shift, the effect of solvent polarity on the compounds' emission maxima was minimal in all the solvents studied (Tables 1 and S6). This indicates that the states initially populated by light absorption and those responsible for emission are different. As a result, the Stokes' shifts of all the dyes in polar solvents were considerably larger than those of classical 7-dialkylaminocoumarins, particularly those of the 4-CF_3 derivatives (e.g. 62 nm for **9** *vs* 95 nm for **11** in H_2O).

Coumarins **9** and **10** exhibited excellent Φ_F in less-polar solvents DCM and toluene (0.31-0.70), while its Φ_F decreased in polar protic and non-protic polar solvents (0.10-0.18). Fluorescence quenching in polar solvents might be a consequence of the formation of a twisted intramolecular charge transfer (TICT) excited state, which should be more stable in polar media.[20,21] TICT states are known to relax rapidly by non-radiative decay pathways, thereby decreasing the fluorescence yields in polar media. For **9-12**, this hypothesis was supported by the observation of Φ_F enhancement in glycerol compared to methanol (Table S6). These two solvents have similar polarity and only the high viscosity of glycerol could prevent the twisting out of the 7-alkylamino group out of the coumarin plane, thereby reducing the formation of the TICT and enhancing the fluorescence yield.[22] Further confirmation was obtained by time-resolved fluorescence spectroscopy, where the fluorescence lifetime was found to be longer in less-polar and viscous solvents, indicating that the competing deactivation channel has been arrested (Figure S20). Despite its decrease in polar solvents, it is worth noting that Φ_F of dyes **9** and **10** are still higher (e.g

Φ_F=0.15 for **9** in H_2O) than those of the unmodified coumarin **1** (e.g. Φ_F=0.058 in H_2O)[21c] or even of the parent dicyanocoumarin derivative **3** (e.g. Φ_F=0.05 for **3**[13] *vs* Φ_F=0.15 for **9** in MeOH). Thus the replacement of one cyano group in **3** by *N*-alkylpyridinium not only red-shifts its absorption and emission but it also improves the photophysical parameters relevant for cell imaging purposes, such as Stokes' shift, Φ_F and brightness.

Table 1. Photophysical data of the coumarin derivatives 9-12 in different solvents.

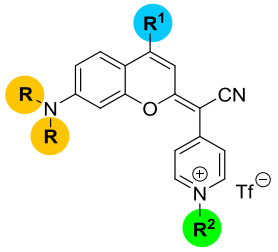

R / R^1	compd	R^2	Solvent	λ_{abs} (nm)	ε ($mM^{-1}cm^{-1}$)	λ_{em} (nm)	Stokes Shift (nm)	Φ_F	τ_F (ns)
R = Et R^1 = CH_3	**9**	CH_3	H_2O	543	31	605	62	0.15	1.0
			ACN	548	75	609	61	0.18	1.4
			DCM	569	67	607	38	0.70	5.4
	10	CH_2CF_3	H_2O	562	33	631	69	0.026	0.5
			ACN	567	43	636	69	0.12	1.2
			DCM	588	51	628	40	0.31	2.9
R = Me R^1 = CF_3	**11**	CH_3	H_2O	567	13	662	95	0.019	0.3
			ACN	569	47	668	99	0.023	0.2
			DCM	600	34	657	57	0.054	0.7
	12	CH_2CF_3	H_2O	595	6.9	683	88	0.046	0.5
			ACN	597	26	689	92	0.12	1.4
			DCM	621	24	679	58	0.25	3.5

In the case of the 4-CF_3 series (**11-12**), Φ_F were reduced with respect the 4-CH_3 analogues, even in non-polar solvents such as DCM (e.g. 0.25 for **12** *vs* 0.70 for **9**), which led to even lower values in polar solvents (e.g. 0.05 in water for **12**). This is not a surprising result since the introduction of strong electron-withdrawing groups like CF_3 in coumarin or xanthene derivatives[9b,16] is known to generate dyes with longer absorption and emission wavelengths, but with reduced Φ_F, a phenomenon that typically occurs

with NIR fluorescent dyes. Even so, the Φ_F of **11** and **12** in glycerol were considerably higher (Φ_F=0.16 for **11** and 0.26 for **12**; Table S6), which suggests that if TICT formation could be prevented this would further improve the Φ_F of COUPY scaffolds emitting in the far-red/NIR region.

Finally, the photostability of **9-12** coumarins in water was studied under green LED irradiation (520 ± 18 nm; Figure S22). Although for **12** the incorporation of the two CF_3 moieties decreases it photostability, the other COUPY dyes (**9-11**) are photostable up to light fluences larger than 20 J/cm^2, which are more than one order of magnitude above typical fluences used for cell imaging purposes.[2d]

To summarise, the introduction of a pyridinium moiety in COUPY scaffolds changes the accepted vision of the photophysics of coumarins dyes (panel A in Figure 4).[18] Thus, in conventional coumarins, photoexcitation leads to a charge transfer state that is stabilized in polar solvents, leading to both red-shifted absorption and emission. By contrast, the ground state of COUPY dyes **9-12** is slightly more polar than the excited state (see Table S4 and Figure S13), leading to blue-shifts in the absorption spectra. However, the position of the emission wavelength is essentially insensitive to the solvent polarity, indicating that no substantial dipole moment changes occur (panel B in Figure 4). As a result, COUPY dyes show larger Stokes' shifts in polar solvents, which adds them potential value for fluorescence imaging applications. In both cases, formation of TICT states in polar solvents leads to faster non-radiative decay of the excited state, which can be arrested by increasing the solvent viscosity.

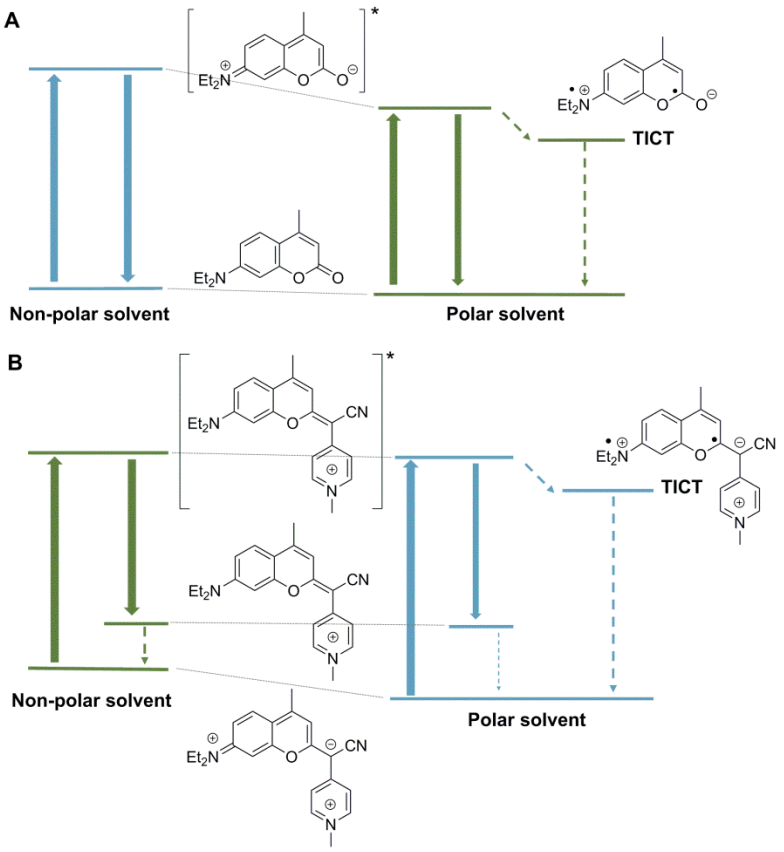

Figure 4. Distinct solvatochromism in (A) conventional coumarins and (B) the new COUPY dyes, as exemplified with compounds **1** and **9**.

Fluorescence imaging of COUPY dyes in living cells

Once demonstrated the promising photophysical properties of the fluorescent dyes based on COUPY scaffolds, we investigated their potential applications for cellular imaging. First, the cellular uptake of coumarin **9** was studied in HeLa cells by confocal microscopy by irradiation with a yellow light laser (λ_{ex} = 561 nm). To our delight, fluorescence after 20 min of incubation was clearly observed in different cellular organelles confirming uptake by cells. At 0.5 and 1 μM of coumarin **9** (Figure 5A,B respectively), mitochondria and intracellular vesicles were stained and also -although less intense- the nucleoli. At 2 μM (Figure 5C) the same pattern of staining was observed but with higher fluorescence intensity. Similar results were obtained after incubation of HeLa cells with coumarins **10** and **11** (Figure S23), although no significant fluorescence was detected in nucleoli in the case of coumarin **11**, which suggests a higher

preference for mitochondria. Interestingly the fluorescence detected in the mitochondria with coumarin **9** disappeared shortly after continuous irradiation of the cells with the excitation laser (Figure 5D and S23) and left more apparent the staining of nucleoli, cytoplasm and vesicles (see below). Based on the higher red-shifted absorption of coumarin **12**, this dye could be visualized after irradiation with red light (λ_{ex} = 633 nm), although in this case fluorescence was only detected in vesicles inside the cells (Figure S24). The overall results suggest that COUPY dyes have excellent cell plasma and nuclear membrane permeability, and that can be used for bioimaging applications in living cells at a concentration as low as 0.5 μM by incubation with a short period of time.

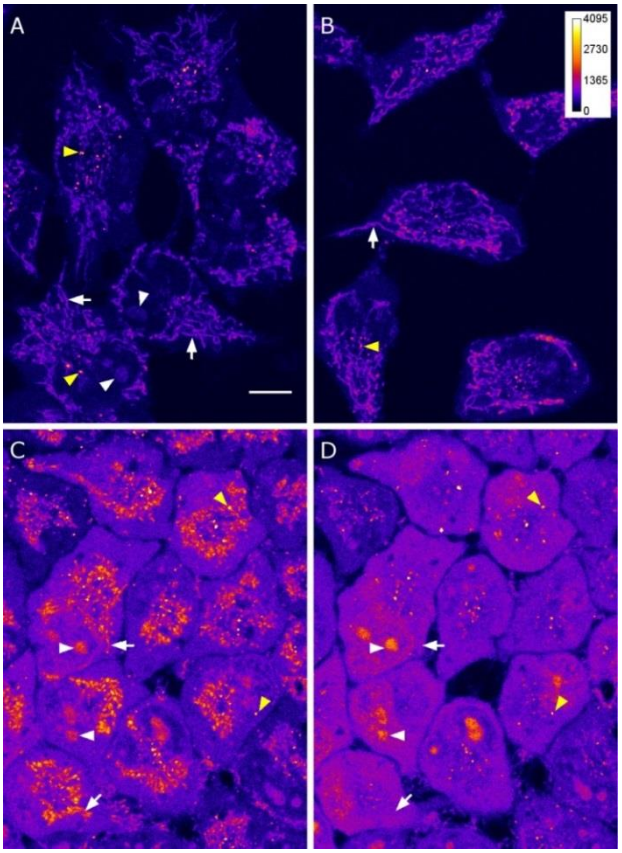

Figure 5. Cellular uptake of coumarin **9**. Single confocal planes of HeLa cells incubated with different concentrations of **9** for 20 min at 37ºC. A) 0.5 μM, B) 1 μM, C and D) 2μM. D) Same cells than in C) after 3 min of 561 nm laser irradiation. White arrows point out mitochondria, white arrowheads nucleoli and yellow arrowheads vesicles staining. All images are colour coded using the Fire lookup table from Fiji (intensity calibration bar in the upper right corner in B). Scale bar: 10 μm. All images are at the same scale.

In order to confirm the subcellular localization of coumarin **9**, we performed co-localization experiments in HeLa cells using specifics markers for mitochondria and nuclei (MitoTracker Green FM and Hoechst 33342, respectively). As shown in Figure 6, the fluorescence emission of coumarin **9** and Mitotracker displayed superimposable distributions, which confirmed that COUPY dyes accumulate into the mitochondria. Similar results were obtained from co-localizations experiments with coumarins **10** and **11** and MitoTracker Green FM (Figure S25). On the other hand, coumarin **9** detected inside the nuclei was observed where lacked Hoechst staining (Figure 6, arrowheads), thus confirming the accumulation of the compound inside the nucleoli as Hoechst does stain the nucleus but not the nucleolus of cells. These results are good agreement with previous findings on the accumulation of positively-charged fluorophores in these organelles, such as the dicationic bisamidine MitoBlue reported by Vázquez and Mascareñas[23] and other far-red/NIR emitting dyes,[5,9b,15,24] including some pyridinium-containing compounds that accumulate preferably in mitochondria.[25] Examples on the simultaneous localization of far-red/NIR fluorescent dyes in mitochondria and nucleoli are scarce,[15,26,27] particularly of low-molecular weight organic compounds that rapidly and efficiently accumulate in nucleolus.

We next evaluated the photostability of coumarin **9** after incubation in HeLa cells by continuous irradiation with the high-energy laser beam of the confocal microscope (λ_{ex}= 561 nm). Besides good cell membrane permeability, photobleaching (the irreversible destruction of an excited dye) is another important parameter for imaging-related biological applications of fluorophores since it can strongly limit its detectability. As it was previously observed, continuous exposition of coumarin **9** to the excitation wavelength caused the decrease of mitochondria signal after 1-2 min (Figures S23 and S26). This intensity decrease however was followed by an increment of the fluorescence intensity in nucleoli and cytoplasm of cells (see Figures S23 and S26). It is worth noting that this process cannot be attributed to photodegradation of the dye since it was not accompanied by a reduction of the overall fluorescence signal, and suggests diffusion of the unaltered coumarin dye outside the mitochondria upon light stress, which then accumulates in the nucleoli and cytoplasm. By contrast, this re-distribution phenomenon was not observed with **10** and **11** (see Figures S23 and S26). The higher photostability of coumarins **10** and **11**

compared with **9**, particularly that of **11** (see fluorescence bleaching studies in Figure S22), indicates that incorporation of CF_3 groups in COUPY scaffolds at the 4-position of the coumarin skeleton not only allows red-shifting absorption and emission but it also reduces photobleaching considerably. Finally, we also evaluated the retention of coumarin **9** after cell fixation using paraformaldehide (4%) and cell permeabilization using Triton X100. After 10 min of fixation at RT coumarin **9** was not detected in mitochondria although it was still observed in cytoplasm and nucleoli (Figure S27). After cell permeabilization, fluorescence was barely observed (Figure S27).

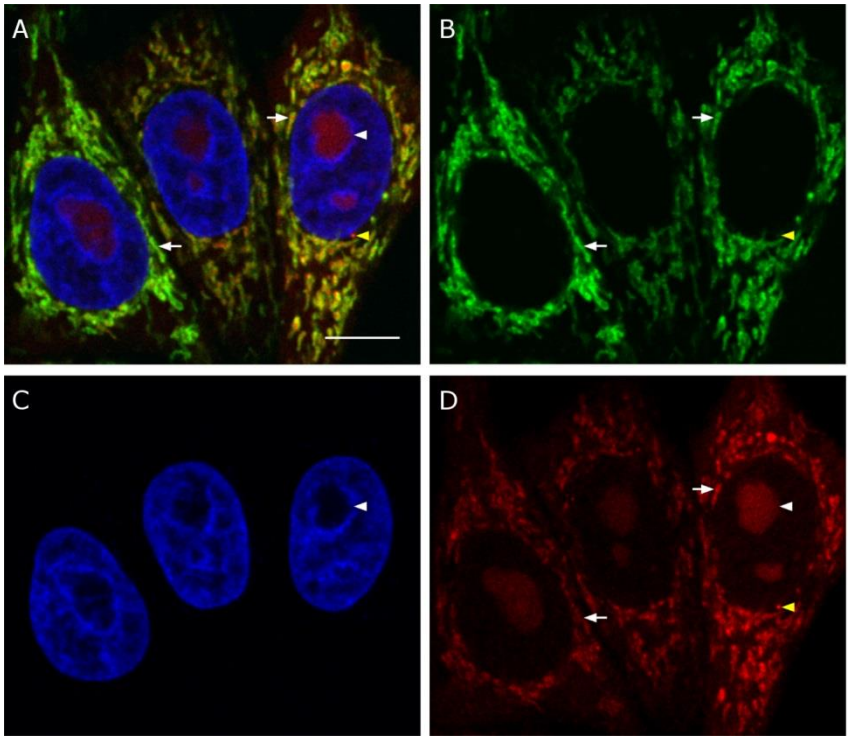

Figure 6. Co-localization studies. Single confocal plane of HeLa cells incubated with coumarin **9** (0.5 μM, red), Mitotracker Green FM (0.1 μM, green) and Hoechst 33342 (1 μg/ml, blue). A) Overlay of the three staining. B), C), D) Mitotracker Green FM, Hoechst 33342 and coumarin **9**, separate staining, respectively. White arrows point out mitochondria, white arrowheads nucleoli and yellow arrowheads vesicles staining. Scale bar: 10 μm.

CONCLUSIONS

In summary, we have developed a novel family of push-pull fluorophores based on novel coumarin scaffolds, nicknamed COUPY, with promising photophysical properties and great potential for cell imaging applications. Such coumarin scaffolds (**7** and **8**) were readily prepared from commercially available precursors (Coumarin 1 and Coumarin 152, respectively) in only two linear synthetic steps, being the key step the condensation of a thiocoumarin derivative with 4-pyridylacetonitrile. Subsequent *N*-alkylation of the pyridine moiety allowed the rapid and efficient synthesis of a novel class of a low-molecular weight fluorophores whose photophysical properties were tuned by selecting the appropriate combination of the *N*-alkylating group (CH_3 or CH_2CF_3) and the substituent at position 4 (CH_3 or CF_3). Notably, COUPY dyes (**9**-**12**) show emission in the far-red/NIR region, large Stokes' shifts in polar media, moderate-to-high fluorescence quantum yields, high photostability, and excellent brightness, which are the result of the re-ordering of the polar and non-polar electronic states as compared to conventional coumarins. Interestingly, NMR spectroscopy revealed the existence of rotamers in solution, and these experimental observations were supported by computational studies. Owing to their low molecular weight, COUPY dyes show excellent cell permeability and accumulate selectively in nucleoli and/or mitochondria of HeLa cells, being their far red/NIR fluorescence emission easily detected at a concentration as low as 0.5 μM.

Taking into account the promising photophysical properties and excellent cell permeability of the fluorophores described in this work, we anticipate that COUPY scaffolds could be used as a basis to synthesize novel NIR-emitting probes with wide biological applications including organelle imaging, biomolecule labelling, cancer imaging and fluorescence-guided surgery. Work is in progress in our laboratory to increase the red-shifted properties of COUPY scaffolds with the aim of shifting absorption and emission into the NIR as well as for improving brightness in aqueous media. This work will be reported in due course.

EXPERIMENTAL SECTION

Materials and Methods

Unless otherwise stated, common chemicals and solvents (HPLC grade or reagent grade quality) were purchased from commercial sources and used without further purification. Aluminium plates coated with a 0.2 mm thick layer of silica gel 60 F_{254} were used for thin-layer chromatography analyses (TLC), whereas flash column chromatography purification was carried out using silica gel 60 (230-400 mesh). Reversed-phase high-performance liquid chromatography (HPLC) analyses were carried out on a Jupiter Proteo C_{18} column (250x4.6 mm, 90 Å 4 μm, flow rate: 1 mL/min) using linear gradients of 0.045% TFA or 0.1% formic acid in H_2O (A) and 0.036% TFA or 0.1% formic acid in ACN (B). NMR spectra were recorded at 25 ^oC in a 400 MHz spectrometer using the deuterated solvent as an internal deuterium lock. Tetramethylsilane (TMS) was used as an internal reference (0 ppm) for ^1H spectra recorded in $CDCl_3$ and the residual protic signal of the solvent (77.16 ppm) for ^{13}C spectra. The residual protic signal of methanol and DMSO was used as a reference in ^1H and ^{13}C NMR spectra recorded in CD_3OD and DMSO-d_6, respectively. Chemical shifts are reported in part per million (ppm) in the δ scale, coupling constants in Hz and multiplicity as follows: s (singlet), d (doublet), t (triplet), q (quartet), qt (quintuplet), m (multiplet), dd (doublet of doublets), dt (doublet of triplets), ddd (doublet of doublet of doublets), br (broad signal), etc. The proton signals of the *E* and *Z* rotamers were identified by simple inspection of the ^1H spectrum and the rotamer ratio was calculated by peak integration. 2D-NOESY spectra were acquired in DMSO-d_6 with mixing times of 300 and 500 ms. The 1D gradient NOE spectra were obtained in a 400 MHz spectrometer using a Gaussian selective pulse and a 0.5 s mixing time with a standard 1D gradient NOE pulse sequence. Electrospray ionization mass spectra (ESI-MS) were recorded on an instrument equipped with single quadrupole detector coupled to an HPLC, high-resolution (HR) ESI-MS on a LC/MS-TOF instrument.

Synthesis and characterization of (coumarin-4-yl)methyl derivatives (7, 9-10).

*2-(Cyano(4-pyridine)methylene)-7-(N,N-diethylamino)-4-methyl-coumarin (**7**).* Compound **2**[13] (1 g, 4.04 mmol) was added to a solution of 4-pyridylacetonitrile hydrochloride (1.25 mg, 8.12 mmol) and NaH (60% dispersion in mineral oil, 2.4 g, 60 mmol) in dry ACN (20 mL) under an Ar atmosphere and

protected from light. After stirring for 2 h at room temperature, silver nitrate (1.45 g, 8.22 mmol) was added and the reaction mixture was stirred at room temperature for 2 h under an Ar atmosphere and protected from light. The crude product was evaporated under reduced pressure and purified by column chromatography (silica gel,0-2% MeOH in DCM) to give 1.19 g of red solid (yield 89%). mp 173-175 ^{o}C; TLC: R_f (10% MeOH in DCM) 0.65. ^{1}H NMR (400 MHz, $CDCl_3$ δ (ppm): (major rotamer) 8.57 (2H, d, *py*, *J* = 6.4 Hz), 7.72 (2H, d, *py*, *J* = 6.4 Hz), 7.32 (1H, d, *H5*, *J* = 9.2 Hz), 6.73 (1H, br q, *H3*, *J* = 0.8 Hz), 6.58 (1H, dd, *H6*, *J* = 9.2 Hz, *J* = 2.4 Hz), 6.44 (1H, d, *H8*, *J*=2.4 Hz), 3.45 (4H, q, *CH_2 Et*, *J* = 7.2 Hz), 2.33 (3H, d, *CH_3*, *J* = 0.8 Hz), 1.24 (6H, t, *CH_3 Et*, *J* = 7.2 Hz). ^{13}C NMR (101 Hz, $CDCl_3$) δ (ppm): (major rotamer) 163.5, 154.4, 150.6, 150.1, 149.8, 144.0, 141.0, 125.4, 120.7, 119.9, 112.3, 109.9, 109.1, 96.9, 81.3, 44.7, 18.4, 12.5. HR-ESI MS, positive mode: *m/z* 332.1761 (calcd mass for $C_{21}H_{22}N_3O$ $[M+H]^+$: 332.1757). Analytical HPLC (30 to 100% B in 30 min, TFA additive: R_t = 13.5 min).

*2-(Cyano((1-methyl(4-pyridin-1-ium)))methylene)-7-(N,N-diethylamino)-4-methyl-coumarin triflate (**9**).* Methyl trifluoromethanesulfonate (48 µL, 0.42 mmol) was added to a solution of **7** (70 mg, 0.21 mmol) in DCM (30 mL). The mixture was stirred overnight at room temperature under an Ar atmosphere and protected from light. After removal of the major part of the solvent, the triflate salt was precipitated with diethyl ether. The product was centrifuged and washed with diethyl ether and vacuum dried to give 96 mg of purple solid (yield 93%). TLC: R_f (DCM) 0.53. ^{1}H NMR (400 MHz, CD_3OD) δ (ppm): (major rotamer) 8.45 (2H, d, *py*, *J* = 7.4 Hz), 8.21 (2H, d, *py*, *J* = 7.4 Hz), 7.73 (1H, d, *H5*, *J* = 9.2 Hz), 7.02-6.96 (3H, m, *H3+H6+H8*), 4.20 (3H, s, *CH_3-py*), 3.61 (4H, q, *CH_2 Et*, *J* = 7.2 Hz), 2.56 (3H, s, *CH_3*), 1.29 (6H, t, *CH_3 Et*, *J* = 7.2 Hz). ^{19}F NMR (376,5 MHz, CD_3OD): -80.2 (3F, s, *Tf*). ^{13}C NMR (101 Hz, DMSO-*d_6*) δ (ppm): (major rotamer) 166.6, 154.7, 152.3, 151.9, 148.5, 143.8, 127.0, 120.7 (q, *J* = 323 Hz, *Tf*), 120.6, 118.3, 111.7, 110.4, 110.2, 96.4, 77.9, 46.0, 44.2, 18.4, 12.4. HR-ESI MS, positive mode: *m/z* 346.1912 (calcd mass for $C_{22}H_{24}N_3O$ $[M]^+$: 346.1919). Analytical HPLC (30 to 100% B in 30 min, TFA additive: R_t = 13.5 min).

*2-(Cyano((1-(2,2,2-trifluoroethyl)(4-pyridin-1-ium)))methylene)-7-(N,N-diethylamino)-4-methyl-coumarin triflate (**10**).* 2,2,2-Trifluoroethyl trifluoromethanesulfonate (80 µL, 0.54 mmol) was added to a solution of

7 (30 mg, 0.09 mmol) in dry ACN (20 mL). The mixture was stirred at 70 ^{o}C during 24 h under an Ar atmosphere and protected from light. Then, most of the solvent was evaporated and the triflate salt of the compound was precipitated with diethyl ether. The product was centrifuged and washed with diethyl ether and vacuum dried to give 40 mg of purple solid (yield 78%). TLC: R_f (DCM) 0.53. ^{1}H NMR (400 MHz, CD_3OD) δ (ppm): (major rotamer) 8.47 (2H, d, *py*, *J* = 7.0 Hz), 8.22 (2H, d, *py*, *J* = 7.0 Hz), 7.78 (1H, d, *H5*, J=8.8 Hz), 7.08-7.04 (3H, m, *H3+H6+H8*), 5.32 (2H, q, *CH_2-CF_3*, *J* = 8.4 Hz), 3.54 (4H, q, *CH_2 Et*, *J* = 7.2 Hz), 2.63 (3H, s, *CH_3*), 1.31 (6H, t, *CH_3 Et*, *J* = 7.2 Hz). ^{19}F NMR (376,5 MHz, CD_3OD): -73.2 (3F, t, *CF_3-CH_2*, *J* = 8.4 Hz), -80.1 (3F, s, *Tf*). ^{13}C NMR (101 Hz, DMSO-d_6) δ (ppm): (major rotamer) 167.2, 155.2, 154.5, 152.4, 150.7, 143.6, 127.3, 123.1 (q, *J* = 280 Hz), 120.7 (q, *J* = 323 Hz, *Tf*), 120.3, 118.0, 112.6, 110.9, 110.6, 96.3, 78.6, 56.4 (q, *J* = 34 Hz), 44.3, 18.5, 12.4. HR-ESI MS, positive mode: *m/z* 414.1788 (calcd mass for $C_{23}H_{23}F_3N_3O$ $[M]^+$: 414.1793). Analytical HPLC (30 to 100% B in 30 min, TFA additive: R_t = 16.1 min).

Synthesis and characterization of (coumarin-4-yl)trifluoromethyl derivatives (6, 8, 11-12).

7-(N,N-Dimethylamino)-4-trifluoromethyl-2-thiocoumarin ***(6)***. 7-(*N*,*N*-Diethylamino)-4-(trifluoromethyl)coumarin (3 g, 11.66 mmol) and Lawesson's reagent (2.65 g, 6.55 mmol) were dissolved in toluene (70 mL) and heated at 100 ^{o}C for 15 h. After evaporation under reduced pressure, the red residue was purified by column chromatography (silica gel, 0-50% DCM in Hexane) to give 2.91 g of a red solid (yield 91 %). mp 169-171 ^{o}C; TLC: R_f (DCM) 0.50. ^{1}H NMR (400 MHz, $CDCl_3$) δ (ppm): 7.53 (1H, dq, *J* = 9.0 Hz, *J* = 2 Hz), 7.17 (1H, s), 6.70 (1H, dd, *J* = 9.0, *J* = 2.8 Hz), 6.68 (1H, d, *J* = 2.4 Hz), 3.10 (6H, s). ^{19}F NMR (376,5 MHz, $CDCl_3$): -63.74 (3F, d, *CF_3*, *J* = 2 Hz). ^{13}C NMR (101 Hz, $CDCl_3$) δ (ppm): 196.0, 159.5, 153.3, 133.0 (q, *J* = 32 Hz), 125.8 (q, *J* = 3 Hz), 122.4 (q, *J* = 275 Hz), 121.0 (q, *J* = 6 Hz), 110.8, 105.2, 97.9, 40.1. HR-ESI MS, positive mode: *m/z* 274.0508 (calcd mass for $C_{12}H_{11}F_3NOS$ $[M+H]^+$: 274.0508).

2-(Cyano(4-pyridine)methylene)-7-(N,N-dimethylamino)-4-trifluoromethyl-coumarin ***(8)***. Compound **6** (700 mg, 2.56 mmol) was added to a solution of 4-pyridylacetonitrile hydrochloride (607 mg, 3.94 mmol) and NaH (60% dispersion in mineral oil, 1.5 g, 37.5 mmol) in dry ACN (25 mL) under an Ar atmosphere

and protected from light. After stirring for 2 h at room temperature, silver nitrate (956 mg, 5.63 mmol) was added and the reaction mixture was stirred at room temperature for 2 h under an Ar atmosphere and protected from light. The crude product was evaporated under reduced pressure and purified by column chromatography (silica gel, 0-2% MeOH in DCM) to give 765 mg of red solid (yield 84%). TLC: R_f (DCM) 0.53. ^{1}H NMR (400 MHz, $CDCl_3$ δ (ppm): (major rotamer) 8.66 (2H, m, *py*), 7.74 (2H, m, *py*), 7.43 (1H, dq, *H5*, *J* = 9.2 Hz, *J* = 2 Hz), 7.16 (1H, s, *H3*), 6.61 (1H, dd, *H6*, *J* = 9.2 Hz, *J* = 2.4 Hz), 6.47 (1H, d, *H8*, *J* = 2.4 Hz), 3.12 (6H, s, CH_3). ^{19}F NMR (376,5 MHz, CD_3OD): -64.2 (3F, br s, CF_3). ^{13}C NMR (101 Hz, $CDCl_3$) δ (ppm): (major rotamer) 160.5, 154.8, 153.3, 150.3, 139.5, 132.8 (q, *J* = 32 Hz), 126.1, 122.2 (q, *J* = 275 Hz), 121.4, 118.2, 112.6 (q, *J* = 6 Hz), 109.9, 103.8, 97.9, 88.4, 40.4. HR-ESI MS, positive mode: *m/z* 358.1155 (calcd mass for $C_{19}H_{15}F_3N_3O$ $[M+H]^+$: 358.1162). Analytical HPLC (30 to 100% B in 30 min, TFA additive: R_t = 13.4 min).

*2-(Cyano((1-methyl(4-pyridin-1-ium)))methylene)-7-(N,N-dimethylamino)-4-trifluoromethyl-coumarin triflate (**11**).* Methyl trifluoromethanesulfonate (19 μL, 0.17 mmol) was added to a solution of **8** (30 mg, 0.08 mmol) in DCM (20 mL), and the mixture was stirred at room temperature overnight under an Ar atmosphere and protected from light. Then, most of the solvent was removed and the triflate salt of the compound was precipitated with diethyl ether. The product was centrifuged and washed with diethyl ether and vacuum dried to give 36 mg of a purple solid (yield 76%). TLC: R_f (DCM) 0.53. ^{1}H NMR (400 MHz, DMSO-d_6) δ (ppm): (major rotamer) 8.76 (2H, d, *py*, *J* = 7.2 Hz), 8.32 (2H, d, *py*, *J* = 7.2 Hz), 7.54 (1H, dq, *H5*, *J* = 9.2 Hz, *J* = 2 Hz), 7.10 (1H, d, *H8*, *J* = 2.4 Hz), 7.06 (1H, s, *H3*), 7.00 (1H, dd, *H6*, *J* = 9.2 Hz, *J* = 2.4 Hz), 4.28 (3H, s, CH_3-*py*), 3.17 (6H, s, CH_3). ^{19}F NMR (376,5 Mz, CD_3OD): -65.22 (3F, d, CF_3, *J* = 2 Hz), -80.16 (3F, s, *Tf*). ^{13}C NMR (101 Hz, DMSO-d_6) δ (ppm): (major rotamer; the trifluoroacetate salt of the compound was used for recording ^{13}C NMR spectrum) 164.6, 158.0 (q, *J* = 34 Hz, *TFA*), 155.0, 154.0, 146.9, 144.8, 134.6 (q, *J* = 32 Hz), 125.5, 122.6, 121.8 (q, *J* = 276 Hz), 117.1, 116.2 (q, *J* = 296 Hz, *TFA*), 112.1, 109.8 (q, *J* = 5.8 Hz), 103.3, 98.0, 84.3, 46.8. HR-ESI MS, positive mode: *m/z* 372.1315 (calcd mass for $C_{20}H_{17}F_3N_3O$ $[M]^+$: 372.1323). Analytical HPLC (30 to 100% B in 30 min, TFA additive: R_t = 13.1 min).

*2-(Cyano((1-(2,2,2-trifluoroethyl)(4-pyridin-1-ium)))methylene)-7-(N,N-dimethylamino)-4-trifluoromethyl-coumarin triflate (**12**).* 2,2,2-Trifluoroethyl trifluoromethanesulfonate (122 µL, 0.84 mmol) was added to a solution of **8** (50 mg, 0.14 mmol) in dry ACN (20 mL). The mixture was stirred at 70ºC during 24 h under an Ar atmosphere and protected from light. The crude product was evaporated under reduced pressure and purified by column chromatography (silica gel,0-10% MeOH in DCM) to give 38 mg of dark blue solid (yield 46%). TLC: R_f (DCM) 0.53. ^{1}H NMR (400 MHz, CD_3OD) δ (ppm): (major rotamer) 8.74 (2H, d, *py*, *J* = 7.0 Hz), 8.47 (2H, d, *py*, *J* = 7.0 Hz), 7.69 (1H, dq br, *H5*, *J* = 9.2 Hz), 7.28 (1H, s, *H3*), 7.16 (1H, d, *H8*, *J* = 2.4 Hz), 7.09 (1H, dd, *H6*, *J* = 9.2 Hz, J=2.4 Hz), 5.49 (2H, m, CH_2-CF_3), 3.25 (6H, s, CH_3). ^{19}F NMR (376.5 Hz, CD_3OD): -64.98 (3F, s, CF_3), -73.05 (3F, t, CH_2-CF_3, *J* = 8.3 Hz), -80.16 (3F, s, *Tf*).^{13}C NMR (101 Hz, DMSO-d_6) δ (ppm): (major rotamer) 166.0, 155.4, 154.3, 149.6, 144.9, 135.7 (q, *J* = 32 Hz), 125.7, 122.9 (q, *J* = 280 Hz), 122.6, 121.8 (q, *J* = 277 Hz), 120.7 (q, *J* = 323 Hz, *Tf*), 117.0, 113.0, 109.3, 104.0, 98.0, 84.2, 56.9 (q, *J* = 34 Hz), 39.8. HR-ESI MS, positive mode: *m/z* 440.1190 (calcd mass for $C_{21}H_{16}F_6N_3O$ $[M]^+$: 440.1192). Analytical HPLC (30 to 100% B in 30 min, TFA additive: R_t = 15.3 min).

Photophysical characterization of coumarin derivatives 9-12

For the photophysical measurements, all solvents used were spectroscopic grade. Absorption spectra were recorded in a Varian Cary 6000i spectrophotometer (Varian, Palo Alto, CA, USA) at room temperature. Molar absorption coefficients (ε) were determined by direct application of the Beer-Lambert law, using solutions of **9-12** in each solvent with concentrations ranging from 10^{-6} to 10^{-5} M. Emission spectra were registered in a Fluoromax-4 spectrofluorometer (Horiba Jobin-Ybon, Edison, NJ, USA).

Fluorescence quantum yields (Φ_F) were measured by comparative method using cresyl violet in ethanol (CV; $\Phi_{F;Ref}$ = 0.54 ± 0.03) as reference.[28] Then, optically-matched solutions of **9-12** and CV were excited and the fluorescence spectra was recorded. The absorbance of sample and reference solutions was set below 0.1 at the excitation wavelength and Φ_F were calculated using the following equation (1):

$$\phi_{F;Sample} = \frac{Area_{Sample}}{Area_{Ref}} x \left(\frac{\eta_{Sample}}{\eta_{Ref}}\right)^2 x\, \phi_{F;ref} \quad (1)$$

where $Area_{Sample}$ and $Area_{Ref}$ are the integrated fluorescence for the sample and the reference and η_{Sample} and η_{Ref} are the refractive index of sample and reference solutions respectively.

Time-resolved fluorescence decays were registered with a time-correlated single photon counting system (Fluotime 200, PicoQuant GmbH, Berlin, Germany). The samples were excited at 504 nm by means of a picosecond-pulsed LED working at 10 MHz repetition rate. Fluorescence decays were acquired at the emission maxima and they were analyzed using the PicoQuant FluoFit c4.6.5 data analysis software. The counting frequency was kept always below 1%.

The dipoles moments ($\Delta\mu$) differences between the ground (μ_g) and excited states (μ_e) for **9-12** have been estimated from the Lippert-Mataga equation (eq. 2):[29]

$$Stokes\ shift = \bar{\nu}_a - \bar{\nu}_f = \frac{2}{hc{a_0}^3}\ x\ \left(\frac{\varepsilon - 1}{2\epsilon + 1} - \frac{n^2 - 1}{2n^2 + 1}\right)\ x\ \left(\mu_e - \mu_g\right)^2 = \frac{2}{hc{a_0}^3}\ x\ \Delta f\ x\ \Delta\mu^2 \quad (2)$$

where h is Plank's constant, c is the velocity of light, a_0 is the radius of the Onsager cavity around the fluorophore. The parameters ε and n are the solvent dielectric constant and refractive index, respectively, which are grouped in the term Δ_f. The Onsager radius was taken as half of the average distance between the push-pull moieties of the COUPYs fluorophores as described by Mukherjee *et al*.[30]

Photostability studies were performed by monitoring fluorescence bleaching of a 5 μM **9-12** aqueous solution irradiated with green LED light (520 ± 18 nm; 6.7 $mWcm^{-2}$; LED Par 64 Short V2 lamp (Showtec, Kerkrade, Netherlands)).

Cell culture and treatments

HeLa Cells were maintained in DMEM (Dullbecco Modified Eagle Medium) containing low glucose (1 g/L) and supplemented with 10% foetal calf serum (FCS), 50U/mL penicillin-streptomycin and 2 mM *L*-glutamine (everything from Biological Industries). For cellular uptake experiments and posterior observation under the microscope, cells were seeded on glass bottom dishes (P35G-1.5-14-C, Mattek). 24 h after cell seeding, cells were incubated for 20 or 30 min at 37ºC with the required concentration of coumarins **9-12** in supplemented DMEM. Then, cells were washed three times with DPBS (Dulbecco's Phosphate-Buffered Saline, Gibco) to remove the excess of the compounds and kept in low glucose

DMEM without phenol red (Gibco) for fluorescence imaging. Unless otherwise stated, no fixation was carried out.

For co-localization experiments, HeLa cells were treated with **9** (0.5 μM) and MitoTracker Green FM (0.1 μM, Life Technologies) for 30 min at 37ºC in non-supplemented DMEM. After removal of the medium and washing three times with DPBS, cells were incubated for 10 min at 37ºC with Hoechst 33342 (1 μg/ml, Life Technologies) in supplemented DMEM. Finally, cells were washed and kept in low glucose DMEM without phenol red (Gibco) for fluorescence imaging. Co-localization experiments with **10** and **11** were carried out with a higher concentration of dye (2 μM). Quantitative analysis of the co-localization of coumarins **9-11** and MTG resulted in Pearson's correlation coefficients in the order of 0.73-0.80 (SD<0.09).

For fixation studies, HeLa cells were treated with **9** (1 μM) for 30 min at 37ºC. After removal of the medium and washing three times with DPBS, cells were fixed with 4% Paraformaldehyde (Sigma) in PBS for 15 min at room temperature. Then cells were washed again and kept in DPBS for their observation under the microscope. Finally, cells were washed and treated with Triton X100 0.5% in PBS for 10 min at room temperature. Cells were washed and kept again in PBS for their observation under the microscope.

For photostability studies, HeLa cells were incubated with the compounds (2 μM, 30 min at 37ºC) and kept in low glucose DMEM without phenol red (Gibco) for fluorescence imaging.

ASSOCIATED CONTENT

Supporting Information

HPLC traces and UV-Vis absorption and emission spectra of the compounds and results from DFT and fluorescence imaging studies. 1D NMR (1H, ^{13}C and ^{19}F), MS and selected 2D NMR spectra. This material is available free of charge via the Internet at http://pubs.acs.org.

AUTHOR INFORMATION

Corresponding Author

*E-mail: vmarchan@ub.edu

ACKNOWLEDGEMENTS

This work was supported by funds from the Spanish *Ministerio de Economía y Competitividad* (grants CTQ2013-48767-C3-1-R, CTQ2014-52658-R, CTQ2014-55174-P, CTQ2015-71896-REDT and CTQ2016-78454-C2-1-R) and of the Generalitat de Catalunya (SGR2014-987). The authors acknowledge helpful assistance of Dr. Irene Fernández and Laura Ortiz (MS), and Dr. Francisco Cárdenas (NMR) from CCiTUB. The authors acknowledge Dr. Montserrat Terrazas from the Institut de Recerca Biomèdica de Barcelona for supplying HeLa cells. A. G. was a recipient fellow of the University of Barcelona (APIF) and A. N.-H. of the Generalitat de Catalunya (FI-AGAUR). R. B.-O. thanks the European Social Funds and the SUR del DEC de la Generalitat de Catalunya for a predoctoral fellowship (2017 FI_B2 00140).

REFERENCES

(1) (a) Lavis, L. D.; Raines, R. T. *ACS Chem. Biol*. **2008**, *3*, 142–155; (b) Lavis, L. D.; Raines, R. T. *ACS Chem. Biol*. **2014**, *9*, 855-866; (c) Zheng, Q.; Juette, M. F.; Jockusch, St.; Wasserman, M. R.; Zhou, Z.; Altman, R. B.; Blanchard, S. C. *Chem. Soc. Rev*. **2014**, *43*, 1044-1056.

(2) (a) Frangioni, J. V. *Curr. Opin. Chem. Biol*. **2003**, *7*, 626-634; (b) Owens, E. A.; Henary, M.; El Fakhri, G.; Soo Choi, H. *Acc. Chem. Res*. **2016**, *49*, 1731−1740; (c) Guo, Z.; Park, S.; Yoon, J.; Shin, I. *Chem. Soc. Rev*. **2014**, *43*, 16-29; (d) Haque, A.; Faizi, M. S. H.; Rather, J. A.; Khan, M. S. *Bioorg. Med. Chem*. **2017**, *25*, 2017-2034, (e) Wagner, M.; Weber, P.; Bruns, T.; Strauss, W. S. L.; Wittig, R.; Schneckenburger, H. *Int. J. Mol. Sci*. **2010**, *11*, 956-966.

(3) (a) *Handbook of Fluorescent Probes and Research Chemicals*, Spence, M. T. Z., Ed.; Molecular Probes, Inc., Eugene, OR, 9th edition, 2002; (b) Nani, R. R.; Kelley, J. A.; Ivanic, J.; Schnermann, M. J. *Chem. Sci*. **2015**, *6*, 6556-6563; (c) Vendrell, M.; Zhai, D.; Er, J. C.; Chang, Y. T. *Chem. Rev*. **2012**, *112*, 4391-4420.

(4) (a) Mishra, A.; Behera, R. K.; Behera, P. K.; Mishra, B. K.; Behera, G. B. *Chem. Rev*. **2000**, *100*, 1973-2011; (b) Gorka, A. P.; Schnermann, M. J. *Curr. Opin, Chem. Biol*. **2016**, *33*,117-125, (c) Gorka, A. P.; Nani, R. R.; Schnermann, M. J. *Org. Biomol. Chem*. **2015**, *13*, 7584-7598.

(5) Cheng, Y.; Li, G.; Liu, Y.; Shi, Y.; Gao, G.; Wu, D.; Lan, J.; You, J. *J. Am. Chem. Soc*. **2016**, *138*, 4730-4738.

(6) (a) Moliner, F.; Kielland, N.; Lavilla, R.; Vendrell, M. *Angew. Chem., Int. Ed*. **2017**, *56*, 3758-3769, (b) Ong, M. J. H.; Srinivasan, R.; Romieu, A.; Richard, J.-A. *Org. Lett*. **2016**, *18*, 5122-5125.

(7) (a) Long, L.; Li, X.; Zhang, D.; Meng, S.; Zhang, J.; Sun, X.; Zhang, C.; Zhou, L.; Wang, L. *RSC Adv*. **2013**, *3*, 12204-12209; (b) Schill, H.; Nizamov, S.; Bottanelli, F.; Bierwagen, J.; Belov, V. N.; Hell, S. W. *Chem. Eur. J*. **2013**, *19*, 16556-16565; (c) Nizamov, S.; Willig, K. I.; Sednev, M. V.; Belov, V.N.; Hell, S. W. *Chem. Eur. J*. **2012**, *18*, 16339-16348; (d) Nizamov, S.; Sednev, M. V.; Bossi, M. L.; Hebisch, E.; Frauendorf, H.; Lehnart, S. E.; Belov, V. N.; Hell, S. W. *Chem. Eur. J*. **2016**, *22*, 11631-11642.

(8) Roubinet, B; Massif, C.; Moreau, M.; Boschetti, F.; Ulrich, G.; Ziessel, R.; Renard, P. Y.; Romieu, A. *Chem. Eur. J*. **2015**, *21*, 14589-14601.

(9) (a) Chen, J.; Liu, W.; Zhou, B.; Niu, G.; Zhang, H.; Wu, J.; Wang, Y.; Ju, W.; Wang, P. *J. Org. Chem*. **2013**, *78*, 6121-6130; (b) Niu, G.; Liu, W.; Wu, J.; Zhou, B.; Chen, J.; Zhang, H.; Ge, J.; Wang, Y.; Xu, H.; Wang, P. *J. Org. Chem*. **2015**, *80*, 3170-3175

(10) (a) Bochkov, A. Y.; Akchurin, I. O.; Dyachenko, O. A.; Traven, V. F. *Chem. Commun*. **2013**, *49*, 11653-11655; (b) Niu, G.; Liu, W.; Xiao, H.; Zhang, H.; Chen, J.; Dai, Q.; Ge, J.; Wu, J.; Wang, P. *Chem. Asian J*. **2016**, *11*, 498-504.

(11) (a) Fonseca, A. S. C.; Soares, A. M. S.; Goncalves, M. S. T.; Costa, S. P. G. *Tetrahedron* **2012**, *68*, 7892-7900; (b) Fournier, L.; Gauron, C.; Xu, L.; Aujard, Is.; Le Saux, T.; Gagey-Eilstein, N.; Maurin, S.; Dubruille, S.; Baudin, J.-B.; Bensimon, D.; Volovitch, M; Vriz, S.; Jullien, L. *ACS Chem. Biol*. **2013**, *8*, 1528-1536.

(12) (a) Kirpichenok, M. A.; Gorozhankin, S. K.; Grandberg. I. I. *Chem. Heterocycl. Compd*. **1988**, 611-616; (b) Fournier, L.; Aujard, I.; Le Saux, T.; Maurin, S.; Beaupierre, S.; Baudin, J.-B.; Jullien, L. *Chem. Eur. J*. **2013**, *19*, 17494-17507; (c) Yamazoe, S.; Liu, Q.; McQuade, L. E.; Deiters, A.; Chen, J. K. *Angew. Chem., Int. Ed*. **2014**, *53*, 10114-10118; (d) Gandioso, A.; Cano, M.; Massaguer, A.; Marchán, V. *J. Org. Chem*. **2016**, *81*, 11556-11564, (e) Gandioso, A.; Palau, M.; Nin-Hill, A.; Melnyk, I.; Rovira, C.; Nonell, S.; Velasco, D.; García-Amorós, J.; Marchán, V. *ChemistryOpen* **2017**, *6*, 375-384.

(13) Gandioso, A.; Contreras, S.; Melnyk, I.; Oliva, J.; Nonell, S.; Velasco, D.; García-Amorós, J.; Marchán, V. *J. Org. Chem*. **2017**, *82*, 5398-5408.

(14) Fletcher, A. N.; Bliss, D. E. *Appl. Phys*. **1978**, *16*, 289-295.

(15) Corrie, J. E. T.; Munasinghe, V. R. N; Rettig, W. *J. Heterocycl. Chem*. **2000**, *37*, 1447-1455.

(16) Niu, G.; Liu, W.; Zhou, B.; Xiao, H.; Zhang, H.; Wu, J.; Ge, J.; Wang, P. *J. Org. Chem*. **2016**, *81*, 7393-7399.

(17) Hu, D. X.; Grice, P.; Ley, S. V. *J. Org. Chem*. **2012**, *77*, 5198-5202.

(18) Liu, X.; Cole, P. G.; Waddell, P. G.; Lin, T.-C.; Radia, J.; Zeidler, A. *J. Phys. Chem. A* **2012**, *116*, 727-737.

(19) Ravi, M.; Soujanya, T.; Samanta, A.; Radhakrishnan, T. P. *J. Chem. Soc., Faraday Trans*. **1995**, *91*, 2739-2742.

(20) Grabowski, Z. R.; Rotkiewicz, K.; Rettig, W. *Chem. Rev*. **2003**, *103*, 3899-4032.

(21) (a) Grimm, J. B.; English, B. P.; Chen, J.; Slaughter, J. P.; Zhang, Z.; Revyakin, A.; Patel, R.; Macklin, J. J.; Normanno, D.; Singer, R. H.; Lionnet, T.; Lavis, L. D. *Nat. Methods* **2015**, *12*, 244-250; (b) Grimm, J. B.; English, B. P.; Choi, H.; Muthusamy, A. K.; Mehl, B. P.; Dong, P.; Brown, T. A.; Lippincott-Schwartz, J.; Liu, Z.; Lionnet, T.; Lavis, L. D. *Nat. Methods* **2016**, *13*, 985-988; (c) Liu, X.; Qiao, Q.; Tian, W.; Liu, W.; Chen, J.; Lang, M. J.; Xu, Z. *J. Am. Chem. Soc*. **2016**, *138*, 6960-6963, (d) Singha, S.; Kim, D.; Roy, B.; Sambasivan, S.; Moon, H.; Rao, A. S.; Kim, J. Y.; Joo, T.; Park, J. W.; Rhee, Y. M.; Wang, T.; Kim, K. H.; Shin, Y. H.; Jung, J.; Ahn, K. H. *Chem. Sci*. **2015**, *6*, 4335-4342.

(22) Haidekker, M. A.; Brady, T. P.; Lichlyter, D.; Theodorakis, E. A. *Bioorg. Chem*. **2005**, *33*, 415-425.

(23) Sánchez, M. I.; Martínez-Costas, J.; Mascareñas, J. L.; Vázquez, M. E. *ACS Chem. Biol*. **2014**, *9*, 2742-2747.

(24) Zheng, K.; Lin, W.; Huang, W.; Guan, X.; Cheng, D.; Wang, J.-Y. *J. Mater. Chem. B* **2015**, *3*, 871-877.

(25) (a) Li, C.; Plamont, M.-A.; Aujard, I.; Le Saux, T.; Jullien, L.; Gautier, A. *Org. Biomol. Chem*. **2016**, *14*, 9253-9261; (b) Rosania, G. R. G.; Lee, J. W. J.; Ding, L. L.; Yoon, H.-S. H.; Chang, Y.-T. Y. *J. Am. Chem. Soc*. **2003**, *125*, 1130-1131.

(26) Liu, W.; Zhou, B.; Niu, G.; Ge, J.; Wu, J.; Zhang, H.; Xu, H.; Wang, P. *ACS Appl. Mater. Interfaces* **2015**, *7*, 7421-7427.

(27) Martin, R. M.; Ter-Avetisyan, G.; Herce, H. D.; Ludwig, A. K.; Lättig-Tünnemann, G.; Cardoso, M. D. *Nucleus* **2015**, *6*, 314-325.

(28) Magde, D.; Brannon, J. H.; Cremers, T. L.; Olmsted, J. *J. Phys. Chem*. **1979**, *83*, 696-699.

(29) (a) Lippert, V. E. Z. *Elektrochem*. **1957**, *61*, 962-975; (b) Mataga, N.; Kaifu, Y.; Koizumi, M. *Bull. Chem. Soc. Jpn*. **1956**, *29*, 465-470.

(30) Mukherjee, S.; Chattopdhyay, A.; Samanta, A.; Soujanya, T. *J. Phys. Chem*. **1994**, *98*, 2809-2812.